Jet Algorithms and the Underlying Event

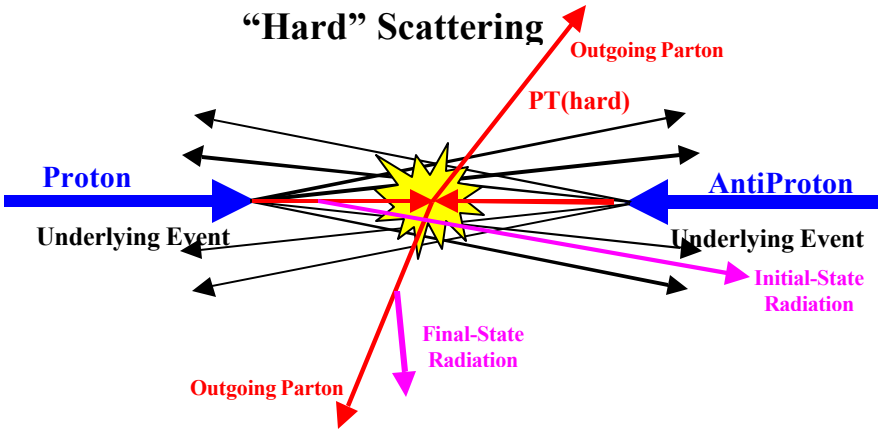

Fig. 1. Illustration of a proton-antiproton collision in which a "hard" 2-to-2 parton scattering with transverse momentum, P_T(hard), has occurred. The resulting event contains particles that originate from the two outgoing partons (plus final-state radiation) and particles that come from the breakup of the proton and antiproton (*i.e.* "beam-beam remnants"). The "underlying event" consists of the beam-beam remnants plus initial-state radiation.

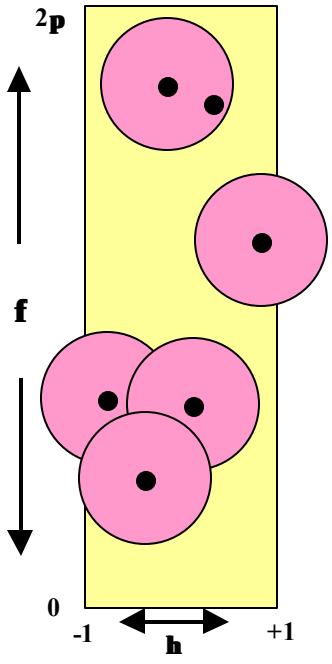

Fig. 2. Illustration of an event with six charged particles (P_T > 0.5 GeV and $|\eta| < 1$) and five charged "jets" (circular regions in η-ϕ space with R = 0.7).

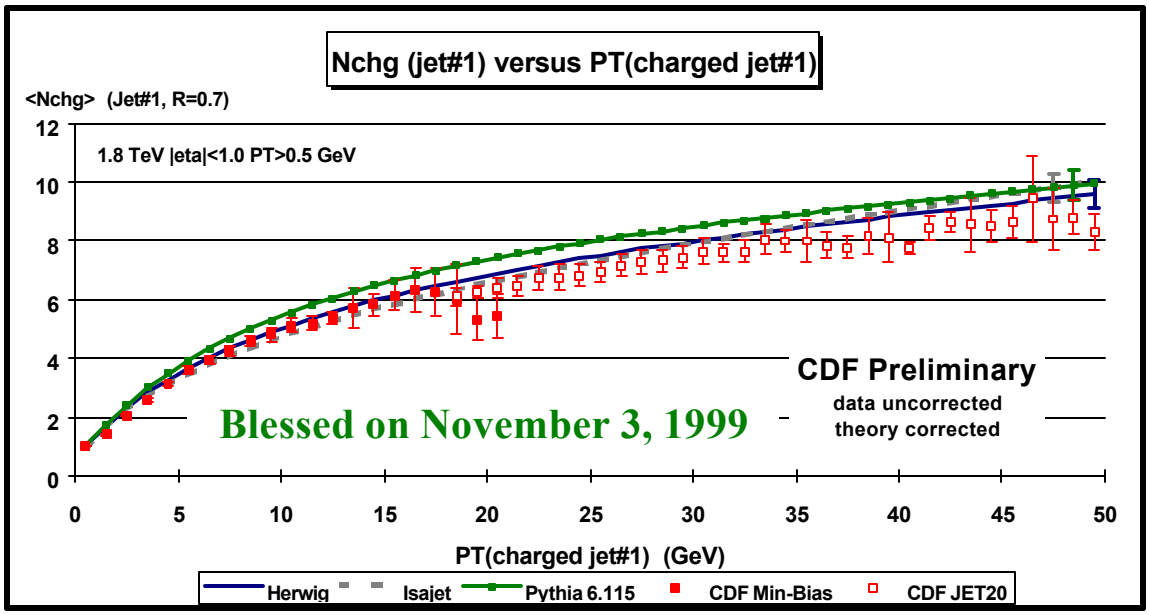

Fig. 3. Plot shows the average number of charged particles (PT > 0.5 GeV, |η| < 1) within the leading charged jet (definition 0) as a function of the PT of the leading charged jet. The solid (open) points are Min-Bias (JET20) data. The errors on the (*uncorrected*) data include both statistical and correlated systematic uncertainties. The QCD "hard scattering" theory curves (Herwig 5.9, Isajet 7.32, Pythia 6.115) are corrected for the track finding efficiency and have an error (*statistical plus systematic*) of around 5%.

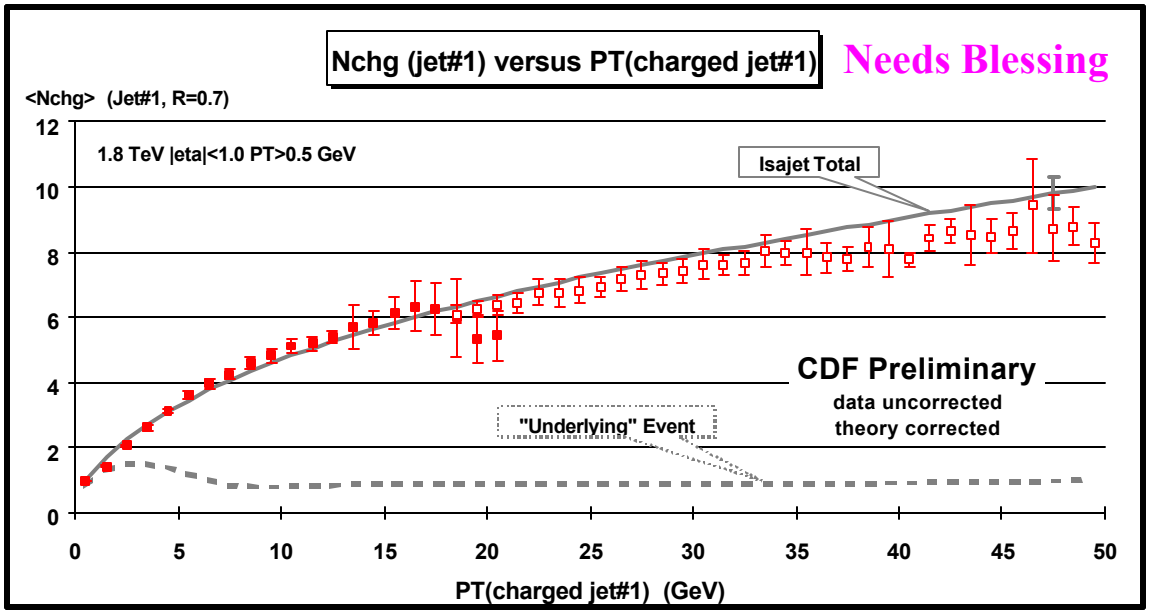

Fig. 4. Data from Fig. 3 on the average number of charged particles (PT > 0.5 GeV, |η| < 1) within the leading charged jet (definition 0) as a function of the PT of the leading charged jet compared with the QCD "hard scatteriing" predictions of Isajet 7.32. Also shown is the contribution from the underlying event (*beam-beam remnants plus initial-state radiation*) predicted by Isajet (see Fig. 1). The errors on the (*uncorrected*) data include both statistical and correlated systematic uncertainties. The theory curves are corrected for the track finding efficiency and have an error (*statistical plus systematic*) of around 5%.

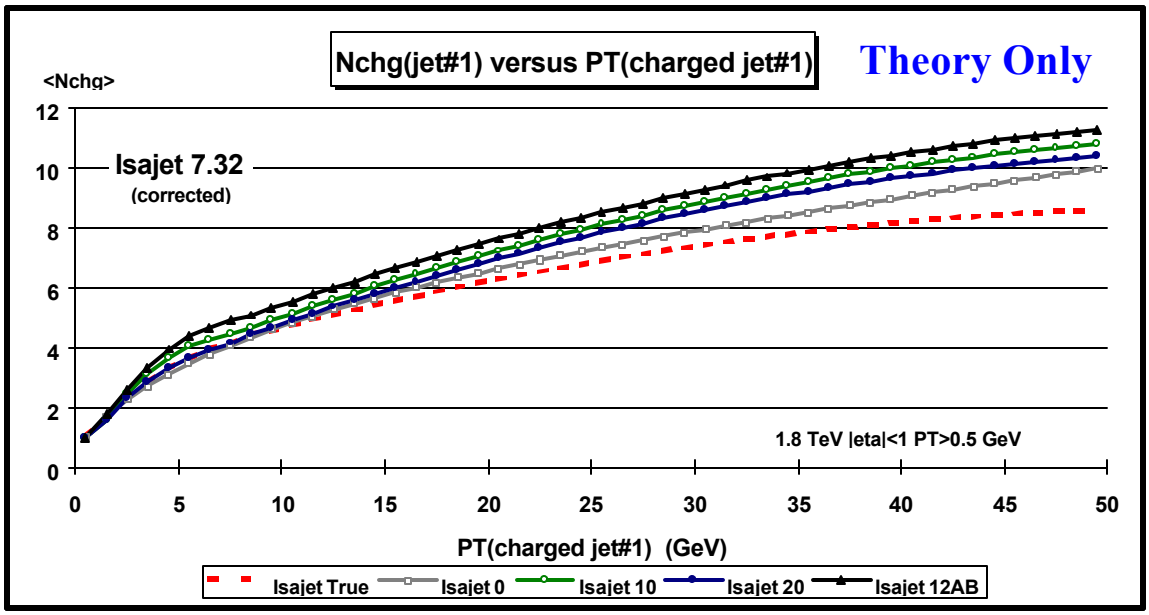

Fig. 5. Shows the average number of charged particles (PT > 0.5 GeV, $|\eta| < 1$) within the leading charged jet as a function of the PT of the leading charged jet resulting from the five jet algorithms in Table 1 applied to QCD "hard scattering" events generated by Isajet 7.32. Note that the five jet algorithms are applied to the *same* set of Isajet events. Also shown are the "true" particles belonging to the leading jet (*Isajet True*) plotted versus the "true" jet PT. The theory curves are corrected for the track finding efficiency and have an error (*statistical plus systematic*) of around 5%.

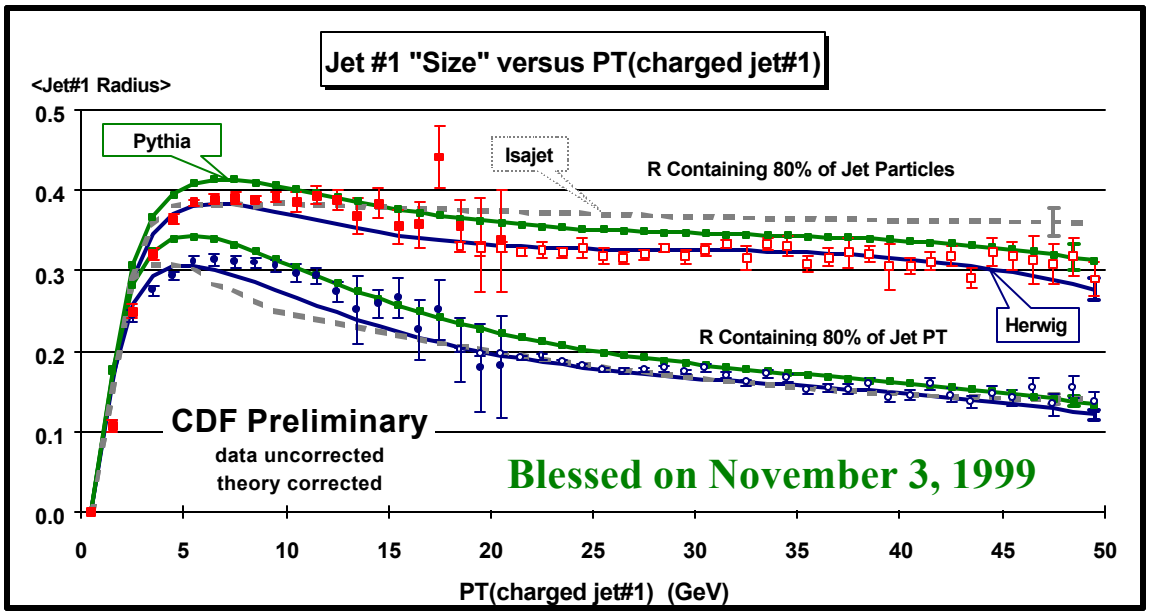

Fig. 6. Plot shows the average radius in η-ϕ space containing 80% of the charged particles (and 80% of the charged P_T) as a function of the transverse momentum of the leading charged jet (definition 0). The errors on the (*uncorrected*) data include both statistical and correlated systematic uncertainties. The QCD "hard scattering" theory curves (Herwig 5.9, Isajet 7.32, Pythia 6.115) are corrected for the track finding efficiency and have an error (*statistical plus systematic*) of around 5%.

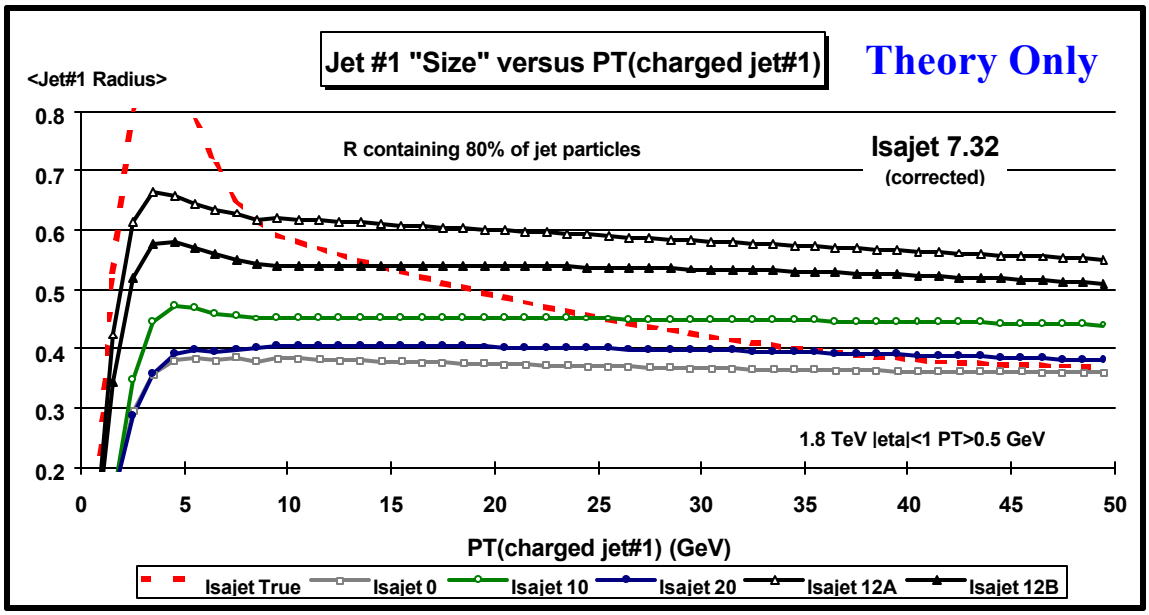

Fig. 7. Plot shows the average radius in η-ϕ space containing 80% of the charged particles as a function of the transverse momentum of the leading charged jet resulting from the five jet algorithms in Table 1 applied to QCD "hard scattering" events generated by Isajet 7.32. Note that the five jet algorithms are applied to the *same* set of Isajet events. Also shown are the "true" particles belonging to the leading jet (*Isajet True*) plotted versus the "true" jet PT. The theory curves are corrected for the track finding efficiency and have an error (*statistical plus systematic*) of around 5%.

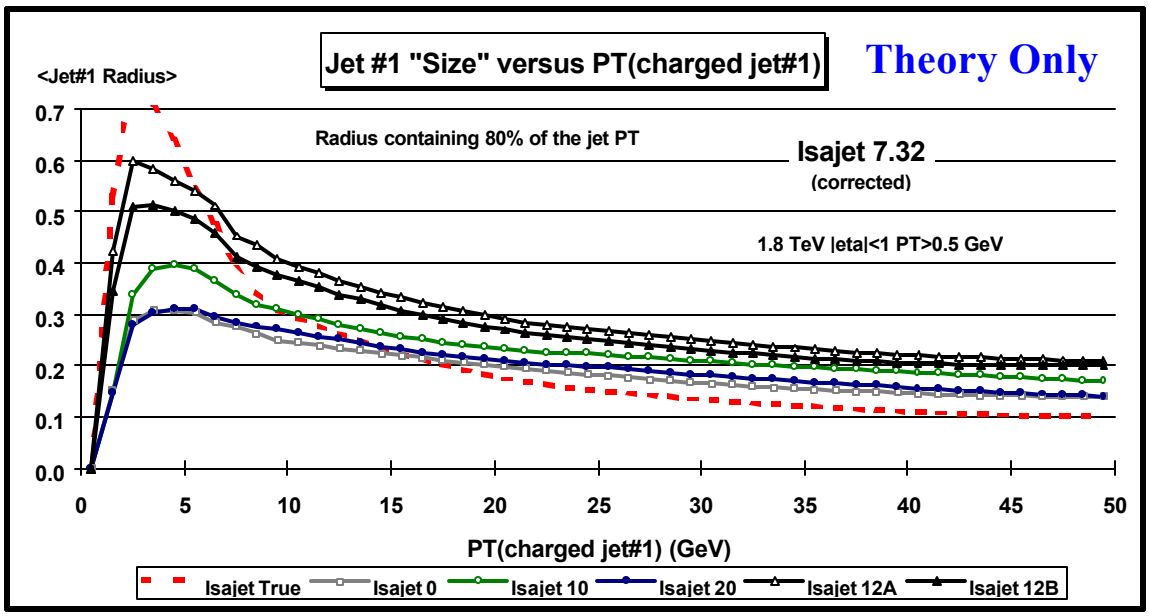

Fig. 8. Plot shows the average radius in η-ϕ space containing 80% of the charged particle *scalar* PT sum as a function of the transverse momentum of the leading charged jet resulting from the five jet algorithms in Table 1 applied to QCD "hard scattering" events generated by Isajet 7.32. Note that the five jet algorithms are applied to the *same* set of Isajet events. Also shown are the "true" particles belonging to the leading jet (*Isajet True*) plotted versus the "true" jet PT. The theory curves are corrected for the track finding efficiency and have an error (*statistical plus systematic*) of around 5%.

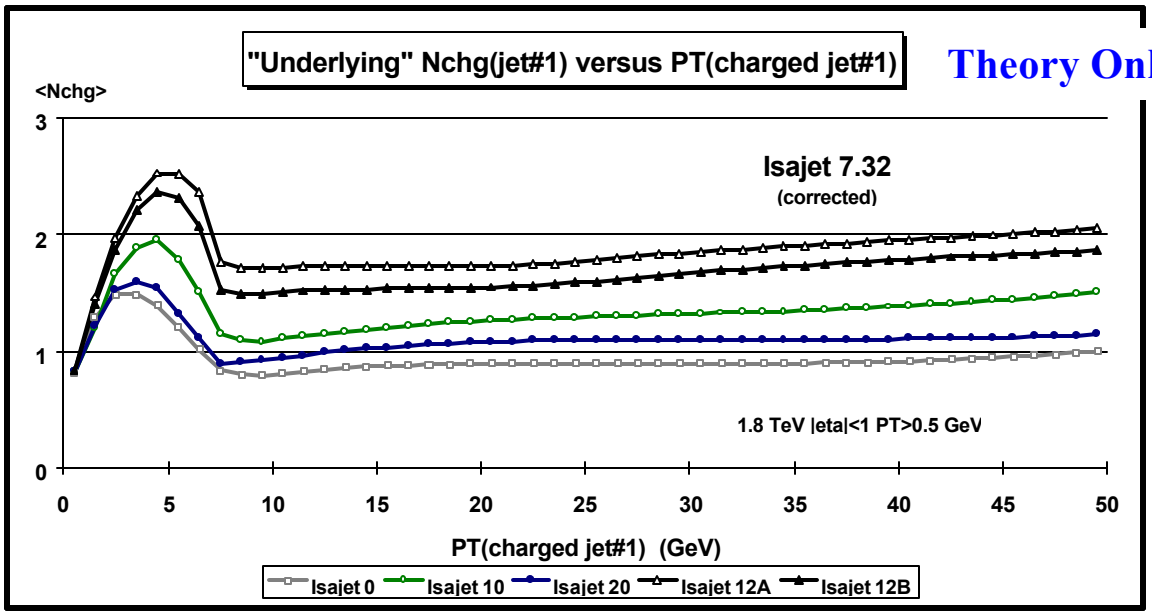

Fig. 9. Shows the contribution to the number of charged particles (PT > 0.5 GeV, $|\eta| < 1$) within the leading charged jet arising from the underlying event (*beam-beam remnants plus initial-state radiation*, see Fig.1) as a function of the PT of the leading charged jet resulting from the five jet algorithms in Table 1 applied to QCD "hard scattering" events generated by Isajet 7.32. Note that the five jet algorithms are applied to the *same* set of Isajet events. The theory curves are corrected for the track finding efficiency and have an error (*statistical plus systematic*) of around 5%.

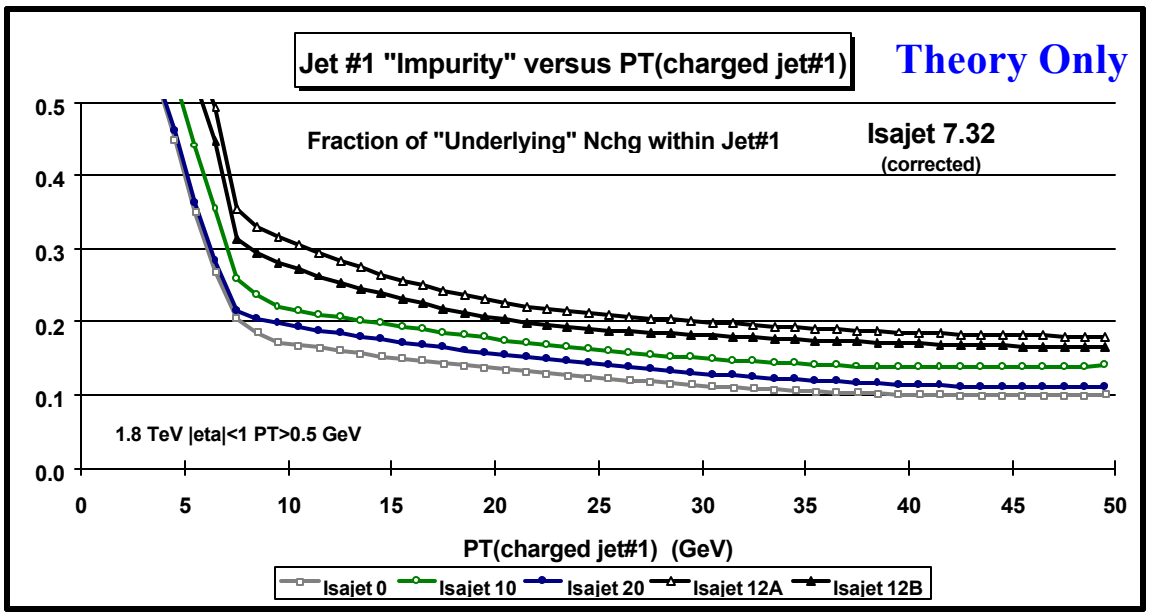

Fig. 10. Shows the fraction of charged particles (PT > 0.5 GeV, $|\eta| < 1$) within the leading charged jet arising from the underlying event (*beam-beam remnants plus initial-state radiation*, see Fig.1) as a function of the PT of the leading charged jet resulting from the five jet algorithms in Table 1 applied to QCD "hard scattering" events generated by Isajet 7.32. Note that the five jet algorithms are applied to the *same* set of Isajet events. The theory curves are corrected for the track finding efficiency and have an error (*statistical plus systematic*) of around 5%.

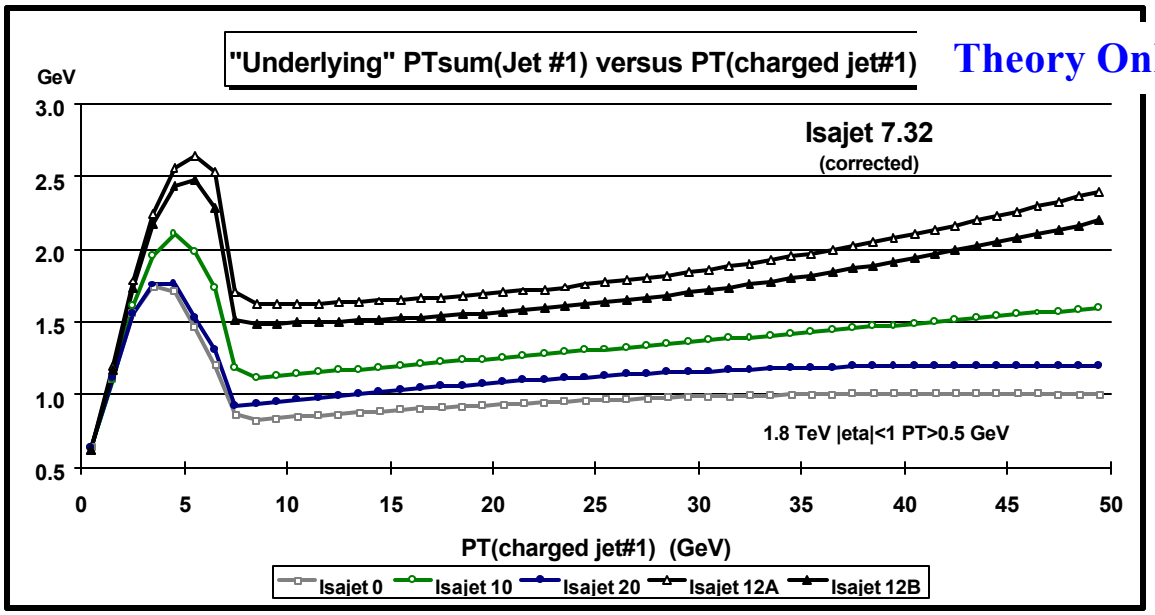

Fig. 11. Shows the contribution to the charged particle scalar PT sum (PT > 0.5 GeV, |η| < 1) within the leading charged jet arising from the underlying event (*beam-beam remnants plus initial-state radiation*, see Fig.1) as a function of the PT of the leading charged jet resulting from the five jet algorithms in Table 1 applied to QCD "hard scattering" events generated by Isajet 7.32. Note that the five jet algorithms are applied to the *same* set of Isajet events. The theory curves are corrected for the track finding efficiency and have an error (*statistical plus systematic*) of around 5%.

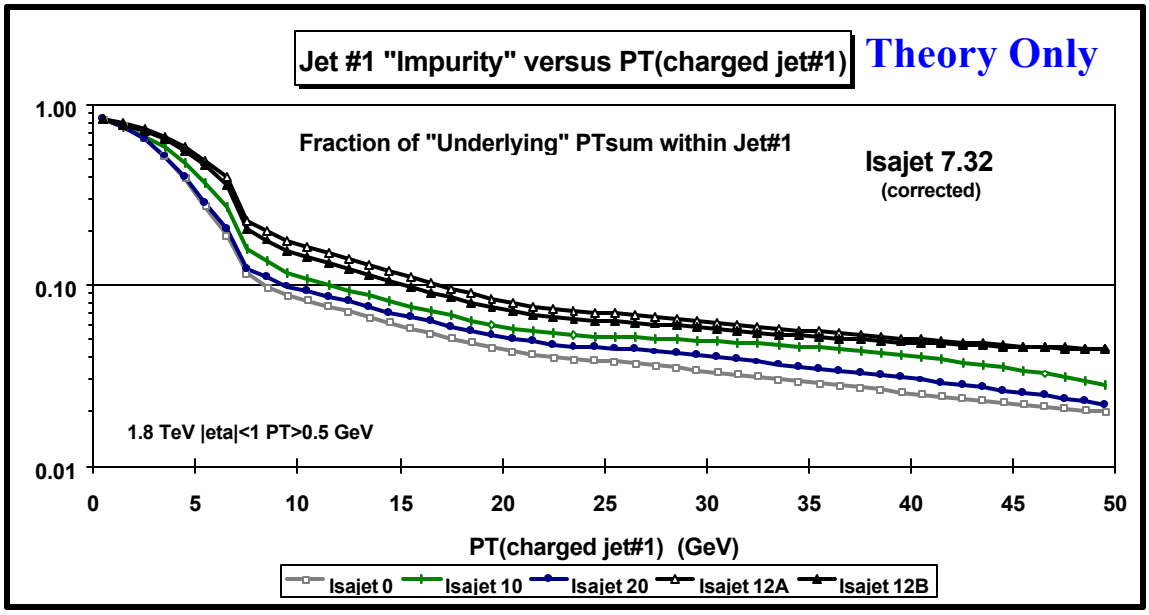

Fig. 12. Shows the fraction of charged particle scalar PT sum (PT > 0.5 GeV, |η| < 1) within the leading charged jet arising from the underlying event (*beam-beam remnants plus initial-state radiation*, see Fig.1) as a function of the PT of the leading charged jet resulting from the five jet algorithms in Table 1 applied to QCD "hard scattering" events generated by Isajet 7.32. Note that the five jet algorithms are applied to the *same* set of Isajet events. The theory curves are corrected for the track finding efficiency and have an error (*statistical plus systematic*) of around 5%.

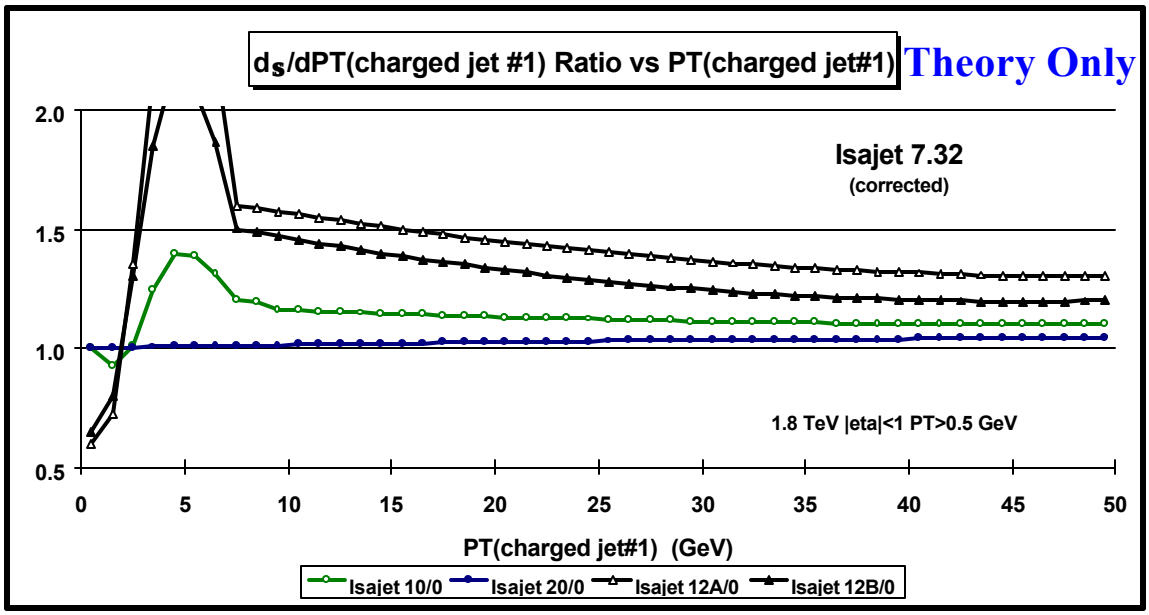

Fig. 13. Shows the charged particle jet cross section, $d\sigma/dPT(jet\#1)$, ratio resulting from the jet algorithms in Table 1 applied to QCD "hard scattering" events generated by Isajet 7.32. The ratios correspond to the leading jet cross sections from definitions 10, 20, 12A, and 12B divided by the leading jet cross section from definition 0. Note that the five jet algorithms are applied to the *same* set of Isajet events. The theory curves are corrected for the track finding efficiency and have an error (*statistical plus systematic*) of around 5%.